Commensurate-Incommensurate Phase Diagrams for Overlayers from a Helical Potts Model

M. Kardar and A. Nihat Berker
Department of Physics, Massachusetts Institute of Technology, Cambridge, Massachusetts 02139
(Received 22 March 1982)

Oversaturated layers such as krypton on graphite are represented by a triplet helical Potts model, incorporating domain walls and antiwalls, and their crossings and annihilations (dislocations). Renormalization-group treatment yields a disordered phase between commensurate and incommensurate phases, down to zero temperature. Coadsorption produces a first-order transition directly between the commensurate and incommensurate phases, in analogy to temper embrittlement.

PACS numbers: 68.45.-v, 64.60.-i, 82.65.Dp, 05.70.Fh

Many adsorbed layers assume a periodicity of their supporting substrate. However, since the adsorbate is smaller than the separation imposed by the substrate, at an increased ambient pressure, commensurability is abandoned. This transition has been subject to many experiments[1-4] and theories,[5,6] with many observations still to be explained. We propose a microscopic model for oversaturated layers, with competing energies straightforwardly related to adatom repulsion and chemical potential. We calculate phase diagrams, and argue for the $(\frac{1}{3})$ power law[2a,3] of the onset of incommensuration. A "temper embrittlement" mechanism is proposed for the first-order transition in coadsorption systems. These results agree with experiments.

Krypton on graphite occupies one of three sublattices of adsorption sites, which are the graphite hexagon centers. The left-hand side of Fig. 1 shows sublattice a occupied. An increased density, due to increased chemical potential μ, can be accommodated as a *heavy domain wall* containing an extra one-third of a column of adsorbates. Its contribution to the Hamiltonian $-\beta\mathcal{H}$ is $l(\mu/3-J)$, where l is the wall length in units of commensurate adatom separation, and the repulsion $J>0$ is the effective nearest-neighbor minus second-neighbor energies. "Effective" is stressed, since the values are modified by adsorption off hexagon centers within a wall width. Actual walls are indeed not sharp, unlike the schematic Fig. 1. In the $\hat{x}$ direction, heavy walls separate (a,b) and cyclic permutations. Alternatively, *superheavy walls*, each accommodating two-thirds of an adsorbate column, separate (a,c) and cyclic permutations. Their contribution to $-\beta\mathcal{H}$ is $l(2\mu/3-2J)$. Equivalent wall identifications are easily done for the other two crystal directions (at $\pm 120°$). Both types of wall are important in the region $\mu/3 \sim J$ of the phenomena of interest. Figure 1 also exhibits heavy and superheavy *wall crossings*, each contributing $-3J/2$ to $-\beta\mathcal{H}$. The two types of wall annihilate at a *dislocation point*, with no additional contribution to $-\beta\mathcal{H}$. Thus, they can also be called wall and antiwall.

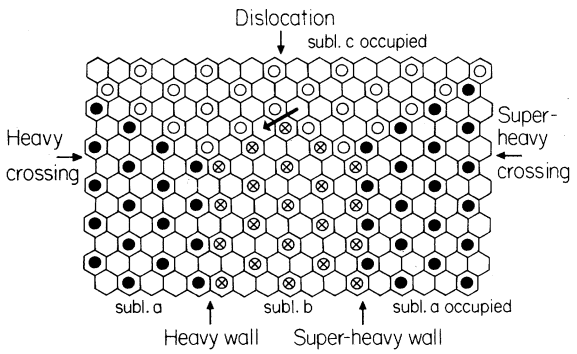

FIG. 1. Structures in an oversaturated layer. A Burgers vector is shown.

The statistical mechanics of the oversaturated layer is carried out by viewing it as composed of hexagonal "patches," each occupying sublattice a, b, or c. Larger domains can be formed by adjoining patches occupying the same sublattice. This procedure generates domain shapes with length scales larger than or equal to l, the side length of the unit hexagonal patch (to be determined self-consistently). Shapes with smaller scales are only approximately accounted, by adding an effective energy $(\frac{1}{2})\ln(l/l_0)$ to each wall intersection (l_0 is the effective wall hard core taken[5] to be 5). This reflects the entropy due to different locations of the intersection, from shape variations on the smaller than l scales. A naive estimate would have used an area $(3\sqrt{3}/2)l^2$ and ignored matching constraints between such areas, giving $2\ln(l/l_0)$. Bak *et al.*[5] have shown the coefficient to be $\frac{1}{2}$ for a system with one type of wall. The precise numerical value of this coefficient is of minor quantitative importance in our calcula-

tions. (A more faithful representation, in future work, would use irregular hexagons with sides l_i.)

Accordingly, a triangular lattice is considered, formed by $\mathfrak{N}$ hexagonal patches of area $(3\sqrt{3}/2)l^2$. We trace over the patch variables $\{s_i = a, b, \text{or } c\}$, to obtain the free energy per adsorption site $\mathfrak{F}(l) = -2/(3\sqrt{3}\,l^2\mathfrak{N})\ln \mathrm{Tr}\exp(-\beta\mathcal{H}_l)$, where $-\beta\mathcal{H}_l = \sum U_l(s_i, s_j, s_k)$ is the extra energy due to wall formation, and the latter sum is over nearest-neighbor triplets, with

$$U_l(a,a,a) = 0 \equiv F,$$

$$U_l(a,a,b) = (l/2)(\mu - 3J) + (\tfrac{1}{2})\ln(l/l_0) \equiv D,$$

$$U_l(a,b,c) = (l/2)(\mu - 3J) + (\tfrac{1}{2})\ln(l/l_0) - 3J/2 \equiv P,$$

$$U_l(a,c,b) = l(\mu - 3J) + (\tfrac{1}{2})\ln(l/l_0) - 3J/2 \equiv N,$$

for down triangles. For up triangles, the last two expressions are interchanged. Minimizing $\mathfrak{F}(l)$, for fixed μ and J, determines l.

The configurations (a,b,c) and (a,c,b) have different "helicities" and occur with different energies. We have thus reached a helical Potts model on a triangular lattice, with three-site interactions. The importance of helicity in incommensuration phenomena has previously been recognized,[7] although motivated differently from here. Helical Potts models on anisotropic square[7] and hierarchical lattices[8] have yielded interesting results. The present model is solved by use of a position-space renormalization-group transformation, in a finite-cluster approximation.[9] Consider the operator[10] τ which leaves one sublattice of the triangular system unchanged, but cyclically promotes the patch variables on the other two sublattices by one and two, respectively: e.g., $\tau(a,b,c) = (a,c,b)$. The Hamiltonian is left invariant under application of τ and simultaneous cyclic permutation of (F,P,N). Our problem was solved in the helically symmetric subspace $P = N$ by Schick and Griffiths.[10] The τ symmetry is sufficient to generalize their recursions to our helically asymmetric space.

The resulting global phase diagram, governed by fifteen fixed points, is shown in Fig. 2. For low values of the dislocation fugacity e^{-D}, ferromagnetic, positive and negative helicity phases are separated by first-order boundaries. At intermediate e^{-D}, a disordered phase at the center is bounded by second-order lines cusped at three bicritical points. At high e^{-D}, two bicritical points disappear, and the disordered phase extends to strong coupling. We shall comment on the possibility of triple and tricritical points in the "bicritical" regions, and of striped phases in the disordered strong-coupling regions.

The phase diagram applicable to layers is in Fig. 3(a). The commensurate phase appears as the ferromagnetic phase of the helical Potts model. The incommensurate phase appears as the negative helicity phase. It is characterized by a hexagonal net of superheavy walls (as distinct from heavy walls, in agreement with experiment[2c]) and by the negative helicity topology of the domains. The disordered (fluid) phase extends down to zero temperature, where the dislocation energy D dominates, between the commensurate and

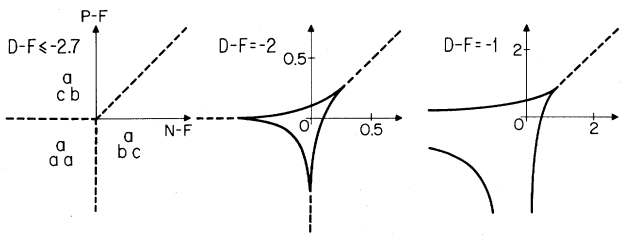

FIG. 2. Global phase diagram of the triplet helical Potts model, from the finite-cluster renormalization. First- (second-) order boundaries are drawn dashed (full).

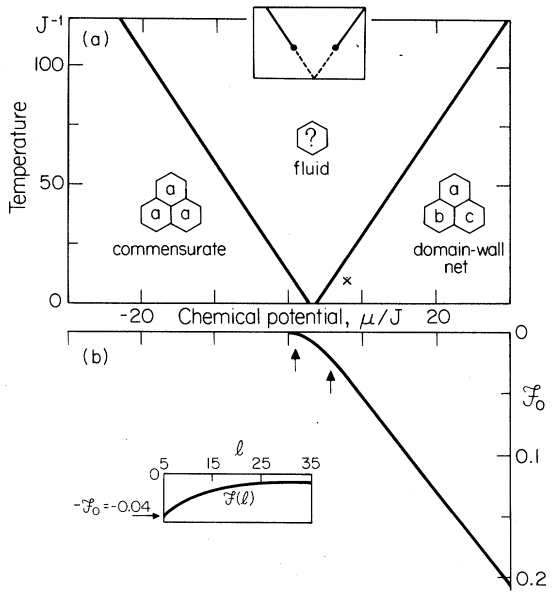

FIG. 3. (a) Overlayer phase diagram. Inset shows possible modification due to the effective vacancy mechanism. (b) The depth $\mathfrak{F}_0$ as chemical potential is scanned at the temperature of the cross. Arrows point to locations of phase transitions. Inset shows $\mathfrak{F}(l)$ at the crossed point in the phase diagram above.

incommensurate phases. This agrees with experiment[2b] and an alternate theoretical approach.[6] The very shallow minima of $\mathcal{F}(l)$, seen (except deep into the incommensurate phase) in Figs. 3(b) and 4 inset, are indicative within our approximation of breathing-mode fluctuations[5] of the wall hexagons.

The incommensuration boundary, between the commensurate and fluid phases, renormalizes to a three-state Potts fixed point. On the fluid side, a large length $\bar{l}$ is introduced into the system, which is the average separation between the wall crossings, which form a disordered fluid. The density n_{cr} of crossings is an even (energylike) density, therefore having the critical exponent $1-\alpha$, where the specific-heat exponent α equals $\frac{1}{3}$ for the three-state Potts model.[11] (To check this even-density exponent $1-\alpha$, we fitted krypton-on-graphite coverage data,[1a] obtaining values between 0.58 and 0.73.) Thus, the misfit should be proportional to $\bar{l}^{-1} \sim n_{cr}{}^{1/2} \sim (\mu-\mu_c)^{(1-\alpha)/2} = (\mu-\mu_c)^{1/3}$, giving an onset exponent which quantitatively agrees with experiments.[2,3] This speculative argument requires that, inside the commensurate phase, wall-crossing fluctuations contribute only to diffuse scattering and/or are of small magnitude. A direct calculation of structure factors is obviously needed in this regard.

A slightly modified approach would recognize that there is less room for adjustment within a superheavy wall than within a heavy wall, so that the effective repulsion J should be higher. Accordingly by use of $\bar{J}=1.2J$ for superheavy walls, the modified phase diagram of Fig. 4 is obtained. It contains a new phase, with a heavy-wall net and domains arranged with positive helicity. A first-order boundary and a multicritical point are also seen. This phase diagram could be expected in experimental systems exhibiting wide walls, where intrawall adjustments are important.

Experiments have also yielded coadsorption of deuterium with krypton on graphite.[4] Our approach indicates this can induce a novel phase diagram: Having a smaller radius than krypton, any deuterium which dissolves into the krypton-rich phases will preferentially go to the superheavy crossings. This is analogous to temper embrittlement in steel, where impurities migrate to grain boundaries.[12] The superheavy crossing then contributes $3(J/2-J_D)+(\mu_D-\mu)$ to $-\beta\mathcal{H}$, where J_D ($<J$) is the deuterium-krypton repulsion, and μ_D is the deuterium chemical potential. By an increase in the ambient partial pressure of deuterium ($\mu_D \gg 1$), this term can be made positive (favorable). Then a bicritical phase diagram is obtained (Fig. 5), a first-order boundary separating the commensurate and incommensurate phases at low temperatures, in agreement with experiment.[4] Conversely, in xenon coadsorption, with radius greater than krypton, solubility is to the interior of domains, stabilizing the commensurate phase.[1b]

Our theory establishes contact with experiments in several aspects. Avenues of further development are also apparent: The inclusion of vacancies will unify the multicritical submonolayer[13]

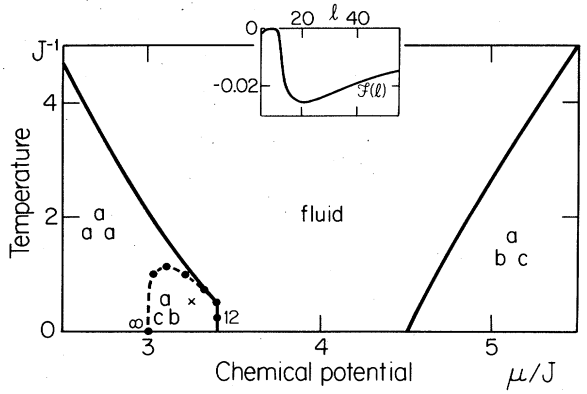

FIG. 4. Phase diagram for $\bar{J}/J=1.2$. Inset shows $\mathcal{F}(l)$ at the crossed point. Such shape occurs in the positive helicity phase and the fluid close to it. At the points consecutively dotted on the boundary, the minima are at $l=12$, 14, 16, 19, 30, 65, ∞. In other regions, $\mathcal{F}(l)$ is as in Fig. 3(b) inset.

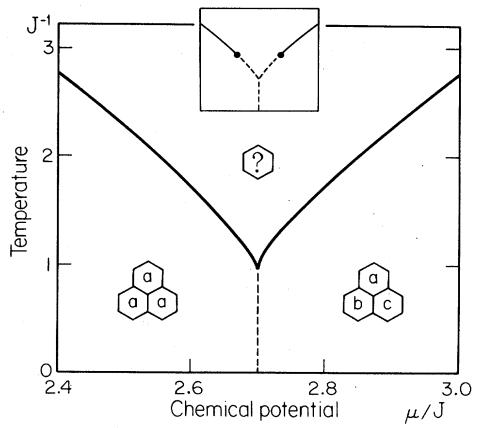

FIG. 5. Coadsorption phase diagram, obtained by changing the sign of the superheavy crossing term. Inset shows possible modification due to the effective vacancy mechanism.

and oversaturated regimes. Moreover, locally disordered regions in Potts models act as effective vacancies, and by condensing cause first-order phase transitions.[14] Effective vacancies are favored by competing helicity (in the fluid dip region of the phase diagram) and could conceivably produce tricritical and triple points [insets Figs. 3(a) and 5]. Finally, by treating triangular patches forming a hexagonal array, the possibility of striped[5a] domain-wall phases would also be included.

We thank R. J. Birgeneau, B. I. Halperin, and P. W. Stephens for helpful conversations. This research was supported by the U. S. Army Research Office under Contract No. DAAG29-81-K002. One of us (M.K.) acknowledges receipt of an IBM Predoctoral Fellowship and one of us (A.N.B.) acknowledges receipt of an A. P. Sloan Fellowship.

[1a]Y. Larher, J. Chem. Phys. 68, 2257 (1978).
[1b]J. Regnier, C. Bockel, and N. Dupont-Pavlovsky, Surf. Sci. 112, L770 (1981).
[2a]P. W. Stephens, P. Heiney, R. J. Birgeneau, and P. M. Horn, Phys. Rev. Lett. 43, 47 (1979).
[2b]D. E. Moncton, P. W. Stephens, R. J. Birgeneau, P. M. Horn, and G. S. Brown, Phys. Rev. Lett. 46, 1533 (1981).
[2c]P. W. Stephens *et al.*, to be published.
[3]S. C. Fain, Jr., M. D. Chinn, and R. D. Diehl, Phys. Rev. B 21, 4170 (1980).
[4]M. Nielsen, J. Als-Nielsen, J. Bohr, and J. P. McTague, Phys. Rev. Lett. 47, 582 (1981).
[5a]P. Bak, D. Mukamel, J. Villain, and K. Wentowska, Phys. Rev. B 19, 1610 (1979).
[5b]J. Villain, Surf. Sci. 97, 219 (1980).
[6]S. N. Coppersmith, D. S. Fisher, B. I. Halperin, P. A. Lee, and W. F. Brinkman, Phys. Rev. Lett. 46, 549 (1981).
[7]S. Ostlund, Phys. Rev. B 24, 398 (1981).
[8]D. A. Huse, Phys. Rev. B 24, 5180 (1981).
[9]M. Schick, J. S. Walker, and M. Wortis, Phys. Rev. B 16, 2205 (1977).
[10]M. Schick and R. B. Griffiths, J. Phys. A 10, 2123 (1977).
[11]M. P. M. den Nijs, J. Phys. A 12, 1857 (1979).
[12]I. Olefjord, Int. Metall. Rev. 4, 149 (1978).
[13]S. Ostlund and A. N. Berker, Phys. Rev. Lett. 42, 843 (1979).
[14]B. Nienhuis, A. N. Berker, E. K. Riedel, and M. Schick, Phys. Rev. Lett. 43, 737 (1979).

Novel *Ab Initio* Correlated Calculations for an Infinite Chain of Hydrogen Atoms

R. D. Poshusta
Chemical Physics Program, Washington State University, Pullman, Washington 99164

and

D. J. Klein
Department of Marine Sciences, Texas A&M University at Galveston, Galveston, Texas 77553
(Received 7 August 1981)

A novel cluster-expanded *ab initio* effective or model Hamiltonian is described and illustrated for a linear chain of hydrogen atoms. The method relies on expanding the model Hamiltonian in a sum of irreducible cluster interaction operators. A hierarchy of increasingly accurate *ab initio* Heisenberg spin Hamiltonians duplicate low eigenvalues of the more complete Schrödinger Hamiltonian. Finally these Heisenberg models are treated to obtain the ground-state energy and magnetic susceptibility of the infinite chain.

PACS numbers: 71.10.+x, 33.10.Cs

Most conventional theories of extended systems rely on a delocalized independent-particle viewpoint. We here show a method which adopts the localized viewpoint (successful in even pre-quantum-mechanical solid-state theories) and combines an expansion in terms of clusters (the localized entities) with *ab initio* correlated calculations on the clusters. This straightforward approach was indicated in low-order approximation for the Hubbard model by Bulaevski.[1] A more detailed description of our method, including its relation to other more conventional approaches, is to be reported elsewhere.[2] Here we illustrate the essential features of our method for one-dimensional chains of hydrogen atoms.

The method combines *ab initio* results for small subunits of an infinite system with a cluster expansion. The *ab initio* calculations may be per-

